+Model
FISH 2210 1–12
ARTICLE IN PRESS

Available online at www.sciencedirect.com
ScienceDirect

ELSEVIER

Fisheries Research xxx (2006) xxx–xxx

FISHERIES RESEARCH

www.elsevier.com/locate/fishres

Remotely sensed local oceanic thermal features and their influence on the distribution of hake (*Merluccius hubbsi*) at the Patagonian shelf edge in the SW Atlantic

J. Wang [a,∗], G.J. Pierce [a], M. Sacau [b], J. Portela [b], M.B. Santos [a,b], X. Cardoso [b], J.M. Bellido [b]

[a] *School of Biological Sciences [Zoology], University of Aberdeen, Tillydrone Avenue, Aberdeen AB24 2TZ, UK*
[b] *Instituto Español de Oceanografía (IEO), Centro Oceanográfico de Vigo, P.O. Box 1552, 36200 Vigo, Spain*

Received 2 December 2005; received in revised form 1 September 2006; accepted 12 September 2006

Abstract

We propose a new index based on sea surface temperature that can be used to locate local oceanic thermal features. The concept of relative spatial variability of local SST (SST RV), and the algorithm used to derive it, are introduced. The utility of this index is compared with that of SST gradient in an analysis of environmental correlates of the distribution and abundance of the hake *Merluccius hubbsi* (Marini, 1933) on the Patagonian shelf edge between 44.5°S and 47.0°S and around the Falkland Islands (Islas Malvinas). The SST RV and SST gradient were calculated from AVHRR SST data. SST RV is suggested to be a more sensitive index than SST gradient for detecting local oceanic thermal features such as fronts. Local hake abundance varied between years and showed strong (albeit complex) relationships with depth and SST, as well as with parameters (SST RV and SST gradient) that indicate the presence of ocean surface thermal features. Although local hake abundance was positively correlated with both SST RV and SST gradient, the former correlation was stronger and in two out of three studied months SST RV was the better predictor of CPUE. Although CPUE tended to increase with SST RV, this relationship breaks down at the highest SST RV values, possibly because hake avoid the most turbulent waters.

Keywords: Hake; SST; Oceanography; Remote sensing; SW Atlantic

1. Introduction

Oceanic circulation has long been known to play an essential role in influencing fish recruitment and distribution. Fish larvae accumulate and primary productivity increases in areas of active regional and local circulation, such as frontal and upwelling areas (either permanent or wind-generated) (Koubbi et al., 1991; Brunet et al., 1992; Olson et al., 1994; Grioche and Koubbi, 1997; Reid, 2001; Beaugrand, 2003; Trathan et al., 2003; González-Quirós et al., 2004; Lafuente et al., 2005). Furthermore, high abundances of many predatory marine resource species, either inshore species or pelagic species, are seen in these areas (Podestá, 1989; Turrell, 1992; Rodhouse et al., 1996; Kimura et al., 1998; Murphy et al., 1998; Cole, 1999; Waluda et al., 1999, 2001; Reid, 2001; Santos, 2000; Zheng et al., 2002, Wang et al., 2003; Sacau et al., 2005).

In the Patagonian shelf area, oceanic circulation is dominated by the Falkland (Malvinas) current and the Brazil current (Fig. 1) (Peterson, 1992; Anderson and Rodhouse, 2001). The Falkland current originates in the northern flow of the Antarctic circumpolar current (ACC) and incorporates the Sub-Antarctic Front, which is the northern boundary of the Antarctic Polar Frontal Zone (APFZ) (Peterson and Whiteworth, 1989). The Falkland current carries cold water of Antarctic origin from the APFZ, and flows northwards along the Patagonian shelf edge to its confluence with the subtropical Brazil current. The latter originates in the South Atlantic gyre, carries warm water and flows south along the Patagonian shelf, at approximately 38°S (Garzoli and Garraffo, 1989).

Sea surface temperature (SST) and SST gradients derived from remotely sensed image have been widely used to depict the existence of regional oceanic circulation features such as fronts,

∗ Corresponding author. Tel.: +44 1224 272459; fax: +44 1224 272396.
E-mail address: j.wang@abdn.ac.uk (J. Wang).

0165-7836/$ – see front matter © 2006 Published by Elsevier B.V.
doi:10.1016/j.fishres.2006.09.010

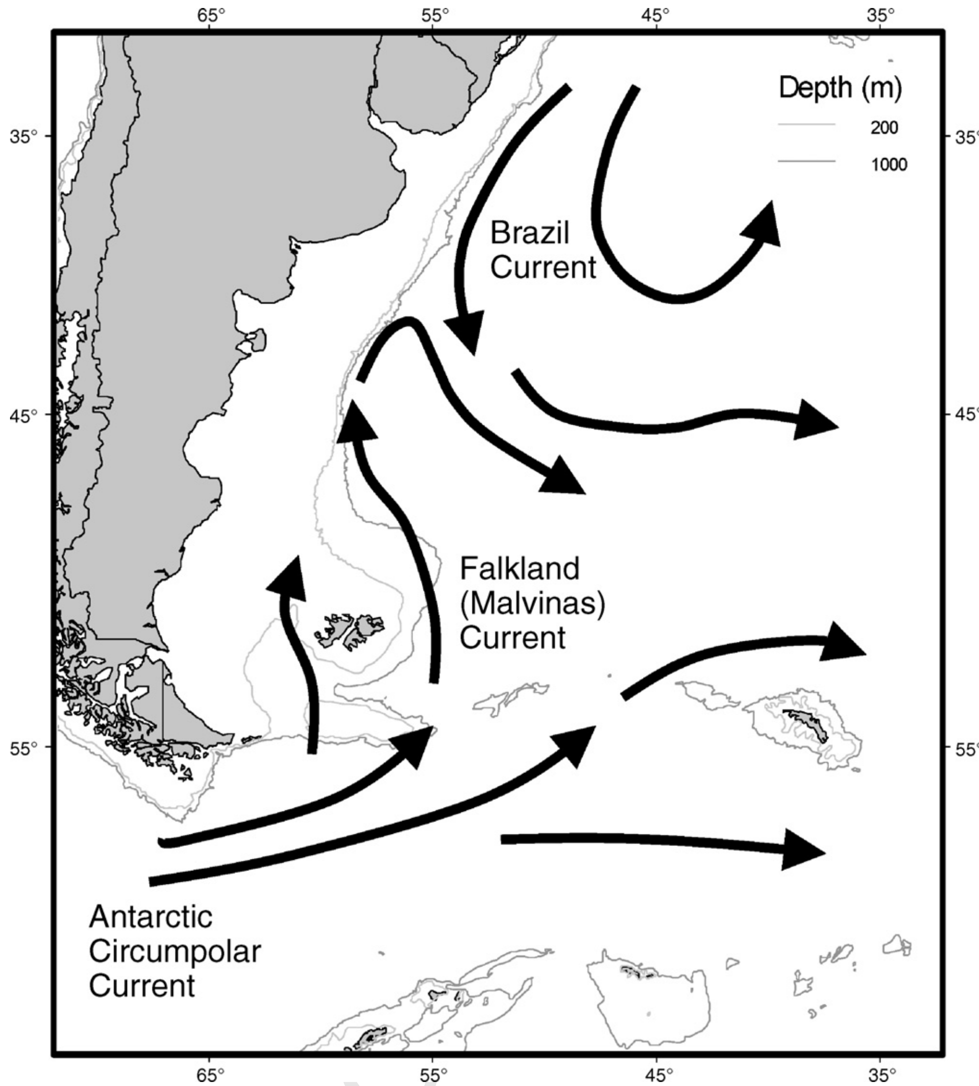

Fig. 1. The major surface oceanic circulation features in the southwest Atlantic (adapted from Anderson and Rodhouse, 2001).

where the SST gradients are higher than in the surrounding area and display consistent or regular changes of direction (Hardman-Mountford and McGlade, 2003). Ullman and Cornillon (2000) presented a method for automated edge-detection of fronts based on the histogram and the gradient algorithm calculated from remotely sensed SST. Valavanis et al. (2005) developed a 'sink' algorithm for detecting oceanic thermal fronts based on remotely sensed SST data. However, the changes in SST and SST gradient within the local oceanic features may be very small, without consistent or regular direction, and may not be easily detected.

The methods mentioned above use either the SST value and/or SST gradient for identifying meso-scale oceanic thermal fronts or locating the edge of meso-scale oceanic thermal fronts. The local variability of sea surface temperature is not considered. However, the value of SST and SST gradients within the areas occupied by the local oceanic thermal features, such as upwellings, and eddies, may not be significantly different from the surrounding areas. Such local oceanic features may not always be identified based on the value of SST and SST gradients. Considering that turbulence occurs within the local oceanic features, the variability of SST may be highest within the area occupied by the local oceanic thermal features. To understand the local variability of SST, a new concept, defined as the relative spatial variability of local SST (SST RV), is introduced. The algorithm for calculating SST RV is presented and used to locate the local oceanic thermal features.

In the present paper we carried out a case study, which focused on the influence of local oceanic thermal features, such as upwellings and gyres (either permanent, wind-generated or due to topography), represented by high values of SST RV and SST gradient, on the spatial distribution of fish abundance. The SST RV and SST gradient are calculated, from remotely sensed AVHRR SST data, and used as indicators for detecting local oceanic thermal features at the Patagonian shelf edge in the SW Atlantic. A comparison of the sensitivity to local oceanic thermal features, between SST RV and SST gradient, is also carried out, to see which is the better indicator.

We chose *Merluccius hubbsi* fishery data from Spanish boats in the case study. The Spanish commercial fishery for hake (*M. hubbsi*) is mainly located in international waters (hereafter

Please cite this article in press as: Wang, J. et al., Remotely sensed local oceanic thermal features and their influence on the distribution of hake (*Merluccius hubbsi*) at the Patagonian shelf edge in the SW Atlantic, Fish. Res. (2006), doi:10.1016/j.fishres.2006.09.010

referred to as “High Seas”) along the shelf edge between 42°S and 48°S, and around the Falkland Islands, where the local oceanography is dominated by the northward flowing Falkland (Malvinas) current. Historically *M. hubbsi* has been one of the most economically important resources in Argentinean waters and it makes up approximately two-thirds of total fish landings in Argentina (Podestá, 1989; Bertolotti et al., 1996; Martínez et al., 1997; Bezzi et al., 2000a,b). Although the Spanish boats carry out *M. hubbsi* fishing by bottom trawling, hake is a bentho-pelagic species and the abundance of hake is thought to be highly associated with oceanic circulation features in the Southwest Atlantic (Podestá, 1989).

The aims of this paper are to present the algorithm for calculation of SST RV, study how suitable it is for detecting local thermal oceanic features and evaluate the influence of local oceanic thermal features on the spatial distribution of fish abundance. The influence of depth and SST on fish abundance are also considered.

2. Methods

2.1. Remotely sensed SST data

Weekly averaged multi-channel sea-surface temperature data (MCSST) derived from the NOAA advanced very high resolution radiometer (AVHRR) were used to detect regional and local oceanic circulation features. These data originate from measurements of emitted and reflected radiance by the 5-channel AVHRR instruments aboard the NOAA-7, -9, -11 and -14 satellites, with a precision of 0.1 °C. Data for both daytime and night-time are available for an equal angle grid with a spatial resolution of 360/2048° per pixel, i.e., the size of a pixel at the equator is 19.55 km × 19.55 km. We downloaded the data from the Physical Oceanography Distributed Active Archive Center, Jet Propulsion laboratory, USA (http://podaac.jpl.nasa.gov). Since diurnal warming affects the estimated SST derived from AVHRR data (Cornillon and Stramma, 1985; Stramma et al., 1986), only night-time data were used in this study.

2.2. Fishery data

Data on hake fishing were collected by observers deployed onboard Spanish trawlers by the Instituto Español de Oceanografía (IEO, Vigo, Spain). The IEO observer programme was established in 1988 to collect fishery and biological data onboard commercial vessels of the Spanish fishing fleet operating in the Southwest Atlantic, with the aim of creating a historical data series to support future assessment and management in specific areas of the Patagonian shelf. Hake total catches (estimated from processed fish by applying conversion factors), fishing efforts, fishing locations, etc, were recorded for each haul. Fig. 2 shows the locations of the recorded hauls from 1989 to 2000.

The activity of the Spanish vessels in the “High Seas” area is restricted to those portions of the continental shelf and slope outside the Argentinean EEZ, i.e. a relatively small area around 42°S, defined as the “north” area, an area between parallels 43°30′ and 48°S, defined as the “middle” area, and the area around the Falkland islands management conservation zones (FICZ and FOCZ), defined as the “south” area (Fig. 2). Fishing is carried out by bottom trawlers and the catches comprise

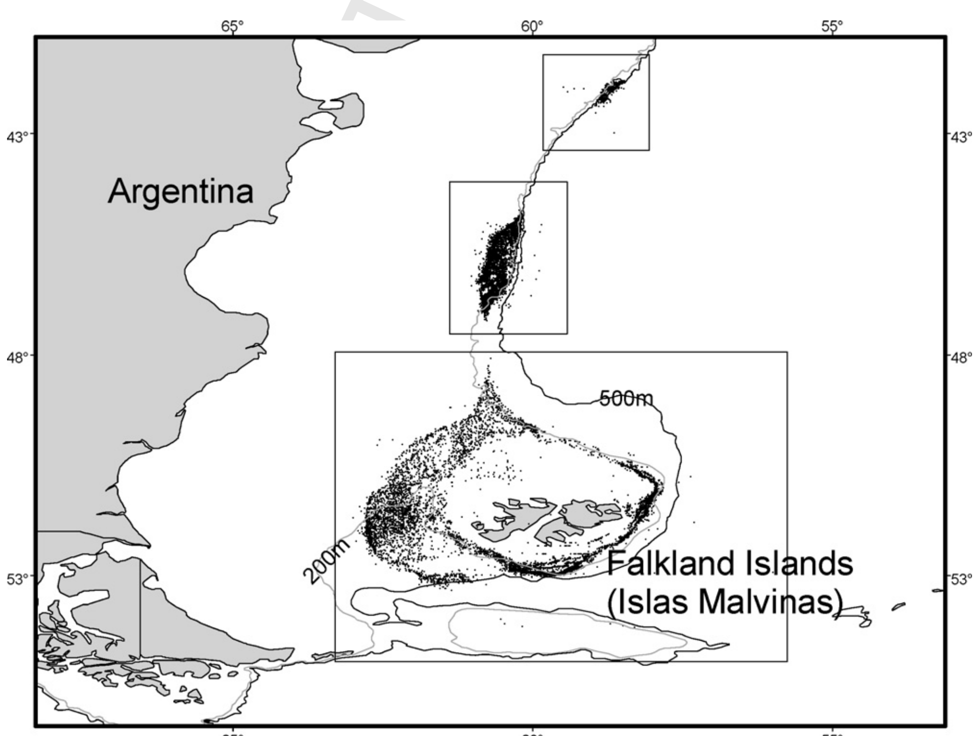

Fig. 2. The locations of the hauls recorded from 1989 to 2000. The Spanish fishery activities are focused on three sub-areas: the north area along the shelf edge around 42°S (the rectangle in the north), the middle area along the shelf edge between parallels 43°30′S and 48°S (the rectangle in the middle), and the south area around the Falkland Islands EEZ (the rectangle in the south).

Please cite this article in press as: Wang, J. et al., Remotely sensed local oceanic thermal features and their influence on the distribution of hake (*Merluccius hubbsi*) at the Patagonian shelf edge in the SW Atlantic, Fish. Res. (2006), doi:10.1016/j.fishres.2006.09.010

both target (hake) and by-catch species. Because there are very few recorded hauls in the north area after 1992, due to a change in the Argentinean EEZ, which reduced the available non-regulated trawling area, this study focused on the middle and south areas. Catch per unit effort (CPUE) of single hauls was used as an abundance index for hake. Because fishing vessels varied with respect to fishing power, we used a standardised CPUE index:

$$\text{CPUE} = \text{catches (kg)} \times [\text{fishing hours} \times (\text{boat engine power (HP)} \times 0.001)]^{-1}.$$

Since the data arise from the hake fishery, it is likely that areas of high hake abundance will be over-represented and it is also possible that CPUE is influenced by local stock depletion due to fishing. Nevertheless, a wide range of CPUE values was recorded and we consider that the data set is adequate for the purposes of the present study.

The observers also recorded the depth of the location of each haul. These depth data were used in analysis. For drawing maps, sea depth contour line data were extracted from general bathymetric chart of the oceans (GEBCO) digital atlas CD-ROM (British Oceanographic Data Centre, National Environmental Research Council).

2.3. Data processing and extracting the information on local thermal oceanic features

Fishery and environmental data were processed and incorporated into a GIS (ArcGIS®, Environmental Systems Research Institute Inc.) and MS Access database. Links were set-up between the different data sets in the GIS and database to allow data overlay for display and analysis. SST gradients and local SST relative variability were calculated from the AVHRR MCSST data, using the GRID module in ArcGIS®.

2.3.1. SST gradients

Conceptually, the slope function fits a plane to the SST values of a 3 × 3 grid-cell neighbourhood around the central cell, using the average maximum technique (Burrough, 1986). The direction in which the plane faces is the aspect value assigned to the central cell. Calculations are based on the percentage SST gradient, defined as the ratio of the difference in SST between two neighbouring cells to the distance between these cells.

2.3.2. Local SST relative variability (RV)

Differing from SST gradient, which quantifies the maximum SST difference between a cell, *i*, and its immediate neighbouring cells (Fig. 3) in a 3 × 3 window, RV is defined as the ratio of the number of cells with different SST values to the total number of cells for which SST values are available, in a 3 × 3 neighbourhood (Fig. 3). Any cell in the grid (other than those cells on the grid boundaries) has 8 immediate neighbouring pixels. Its local relative SST variability is assigned a value of 1/9 = 0.111 if all of the nine cells in the 3 × 3 window have the same SST value, and assigned a value of 1.0 if all of the nine pixels have SST data but the SST value is different in each one (Fig. 3a and b). The

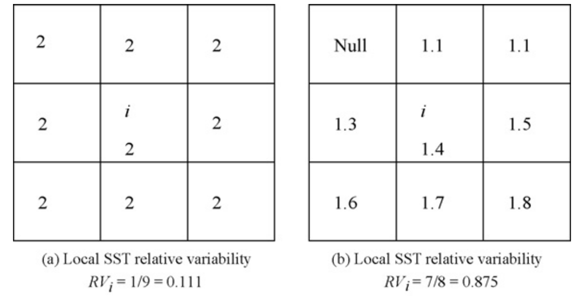

Fig. 3. The local SST relative variability of the pixel, *i*, is defined by the ratio of the number of pixels with different SST values within the 3 × 3 window to the number of pixels having SST values. The figures shows two examples. (a): The pixel, *i*, has the same SST value as its eight immediate neighbouring pixels. Its local SST relative variability, RV_i, is 0.111; (b): the pixel, *i*, and its seven immediate neighbouring pixels have seven different SST values. One immediate neighbouring pixel has no SST value, indicating this pixel represents land surface, or ice, or missing data. The local SST relative variability of the central pixel, RV_i, is 0.875.

value assigned obviously depends on the precision of the SST data used. As the precision of AVHRR MCSST data is 0.1 °C, the smallest SST difference that can be recognized is 0.1 °C.

2.4. Analysis of the relationship between CPUE and surface thermal oceanic features

Considering that the main hake-fishing season is from the Austral autumn to Austral spring, AVHRR SST data sets, covering 1-week periods in April, July and September in each year from 1989 to 2000, were chosen for extracting SST RV and SST gradients. All fishing hauls (i.e. 1392 hauls) from the same periods were selected. Assuming that the standard CPUE can fairly represent the fish abundance, the standard CPUE of each haul, and the SST RV and SST gradient at each haul location were used for analysis (Table 1).

Visual analysis based on GIS and statistical analyses were carried out. Mapping fish abundance of single hauls with a background of the distribution of SST RV or SST gradient was carried out to visualise the hypothesised influence of regional and local oceanic circulation on local abundance of hake. The correlations between the standard CPUE from single hauls and SST RV, SST gradient and depth in the selected 3 weeks in April, July and September from 1989 to 2000 were calculated.

Generalised additive models (GAMs) were constructed using a forwards and backwards stepwise procedure to arrive at the optimum models, which was identified by reference to the AIC (akaike information criterion) and diagnostic plots, e.g. plots of residuals against values of explanatory variables. Degrees of freedom for smoothers were calculated using cross-validation. The response variable was hake CPUE. Where possible transformations were carried out to achieve an approximately normal distribution for CPUE, allowing use of Gaussian GAM, although one data set better fitted an overdispersed Poisson distribution (see Section 3). In the former case the GAMs have identity link functions; in the latter case a log link function is used. The explanatory variables considered were year, SST, SST RV, SST gradient, and depth.

Please cite this article in press as: Wang, J. et al., Remotely sensed local oceanic thermal features and their influence on the distribution of hake (*Merluccius hubbsi*) at the Patagonian shelf edge in the SW Atlantic, Fish. Res. (2006), doi:10.1016/j.fishres.2006.09.010

Table 1
The AVHRR SST data and fishery data used in the analyses

	1989	1990	1991	1992	1993	1994	1995	1996	1997	1998	1999	2000
April												
Day	102	101	100	106	104	103	102	101	106	105	104	103
Hauls	109	75	37	25	37	37	30	53	10	39	40	68
July												
Day	193	193	191	190	195	194	193	192	190	189	194	194
Hauls	48	21	43	36	37	16	15	8	22	21	4	4
September												
Day	256	255	254	253	251	257	256	255	253	252	251	257
Hauls	106	35	49	69	29	40	54	49	43	36	25	26

Three AVHRR SST data in each year were used in analysis. The numbers in the rows labelled "Days" indicate the start day of the weekly averaged SST data. The number in the row labeled "Hauls" is the number of fishing hauls covered by the same period of weekly averaged SST data, and used in the analysis.

3. Results

3.1. Local relative SST variability and SST gradients

Weekly time-series of SST RV and SST gradient data were calculated from AVHRR MCSST data. Figs. 4–6 are examples of maps displaying images of AVHRR SST for days 256–261 of 1989, the calculated SST RV, and SST gradients, respectively. In order to show the main features of the regional oceanic circulation, the maps cover a larger area than the fishing grounds, including the area of the confluence of Falkland (Malvinas) current and the Brazil current. The SST pattern reflects the distribution of the Falkland (Malvinas) current, which carries cold water from south to north, the Brazil current, which carries warm water southwards, and the frontal area where these two currents meet (Figs. 1 and 4).

The spatial distributions of SST RV and SST gradient were rather similar (Figs. 5 and 6). Values of SST RV and SST gradient are both higher in the areas where SST shows bigger changes. However, there are differences, particularly in the area dominated by the Falkland (Malvinas) current from 40°S southwards and with depth less than 500 m. The SST gradient shows much smoother changes than SST RV over this area.

Although, in general, SST RV increases as SST gradient increases, there is substantial variability in SST gradient at each level of SST RV, indicating that changes in SST RV and gradient are not synchronous (Fig. 7). The correlation between SST RV and SST gradient in each of the 3 months is however significant

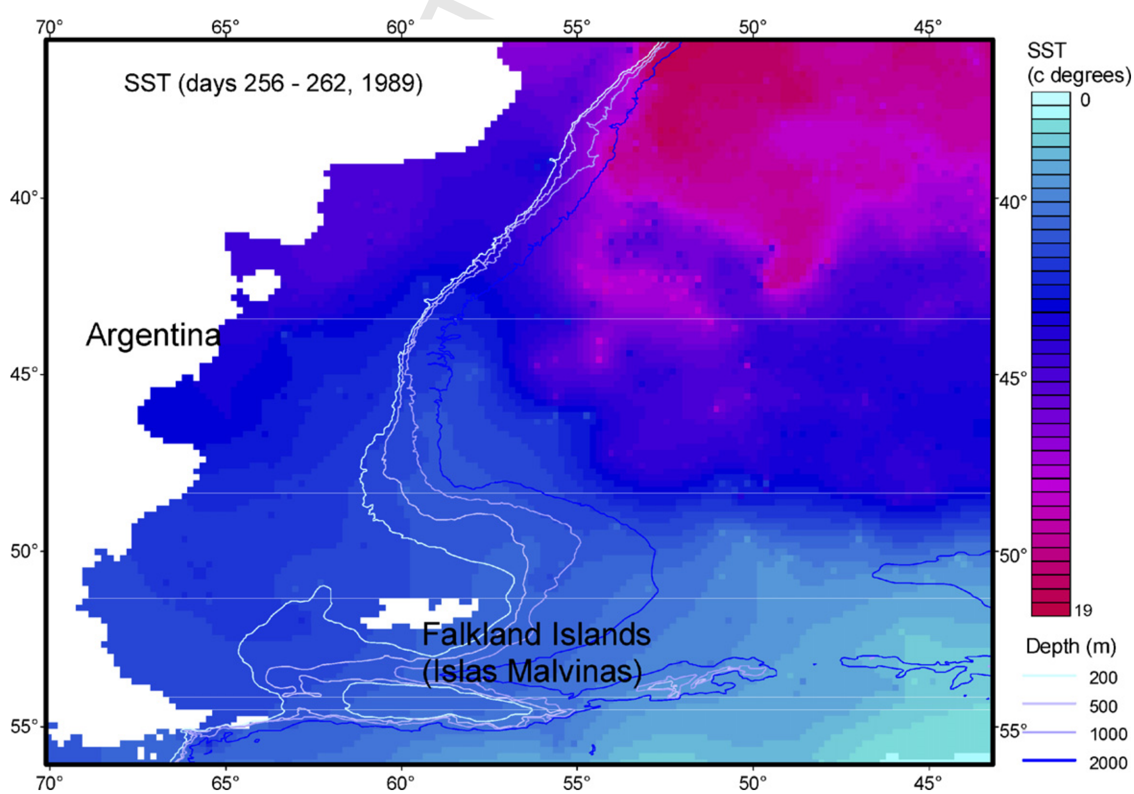

Fig. 4. The display of AVHRR SST data (days 256–262, 1989) with depth contour lines.

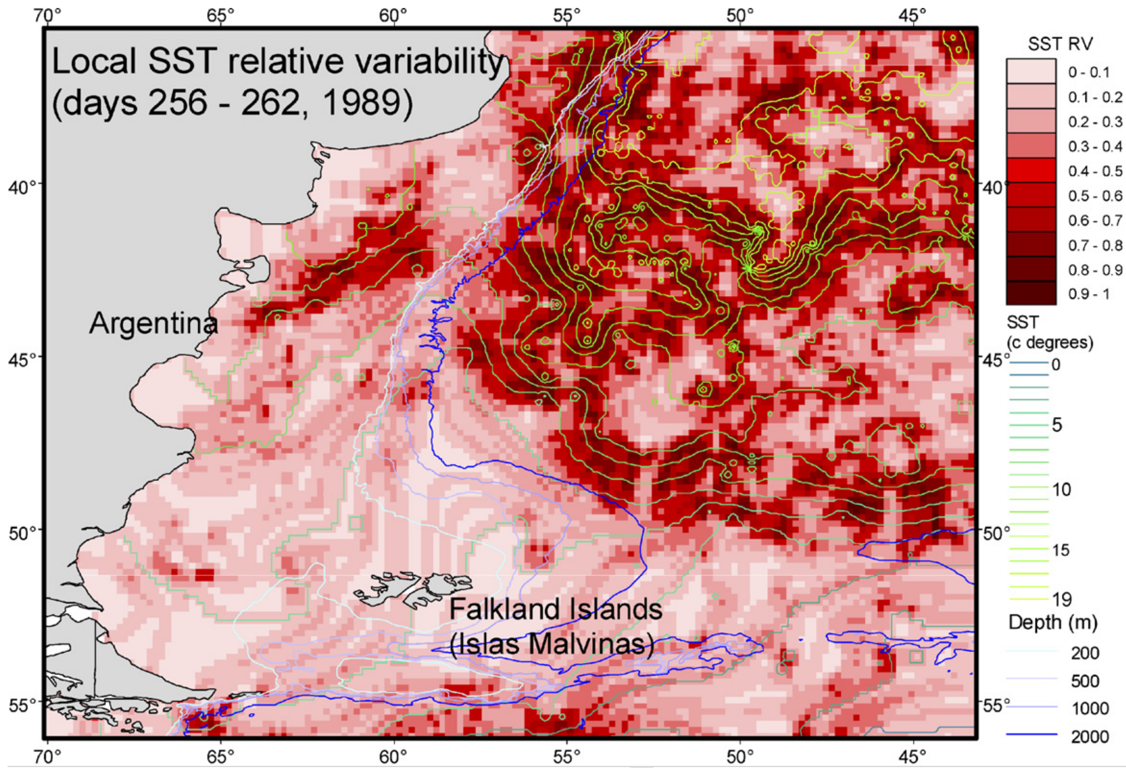

Fig. 5. The display of the local SST relative variability (RV) calculated from AVHRR SST data (days 256–262, 1989) with the background of SST isotherms.

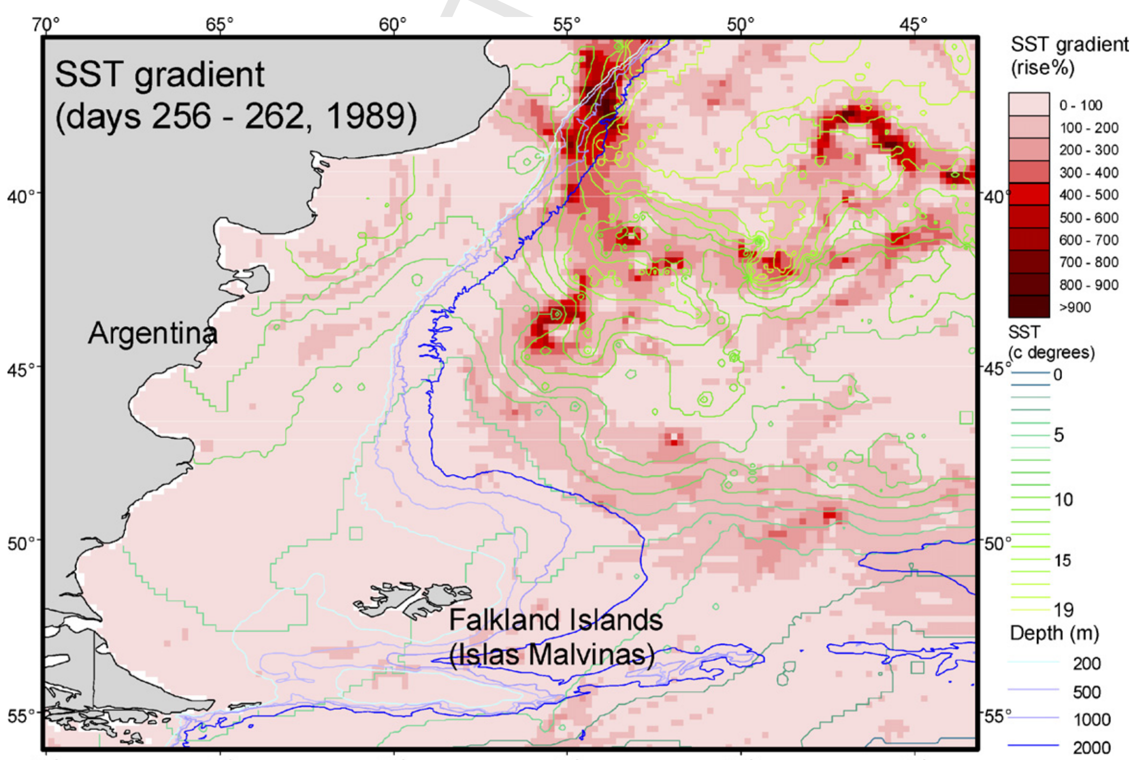

Fig. 6. The display of SST gradients calculated from AVHRR SST data (days 256–262, 1989) with the background of SST isotherms.

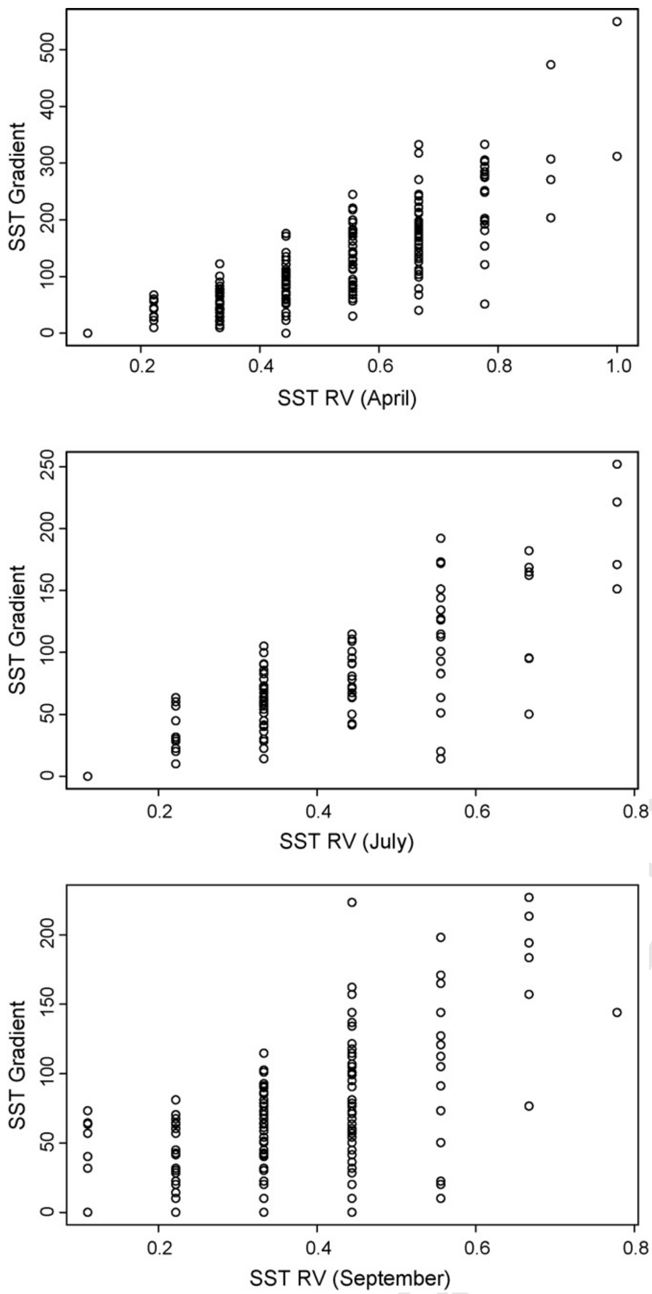

Fig. 7. The pair plots of SST RV and SST gradient in April, July and September.

($r = 0.84$ in April, 0.77 in July, 0.70 in September; $P < 0.001$ in all cases).

3.2. The relationship between fish abundance, SST, SST RV, SST gradients, and depth

As shown in Figs. 8 and 9 most of the hauls with high hake CPUE appear to be located in areas with high SST RV or adjacent to areas with high SST RV, whereas there is no such apparent relationship between CPUE and SST gradient. Compared with Figs. 4–6, Figs. 8 and 9 cover a smaller area, where the main fishing grounds are located. It can be seen that the values for SST gradient in the fishing ground area are generally very low. The hauls with the highest CPUE are located in the area of high local SST RV values, particularly, in the shelf edge area between 45°S and 47°S, and with depth ≤ 200 m.

Correlations of CPUE with SST RV were positive in all 3 months ($P \leq 0.001$, Table 2). The correlation between CPUE and SST gradient was positive in April, weaker in July ($P < 0.05$) and absent in September ($P = 0.277$). In all 3 months, CPUE was strongly negatively correlated with depth.

GAM models were fitted to reveal the relationships between fish abundance and the suite of available environmental variables in each of the three studied months. To minimise the effects of some very high CPUE values, the CPUE data for April were cube-root transformed, which resulted in a symmetrical distribution with rather broad shoulders but otherwise not dissimilar to normal. A Gaussian GAM with identity link function was fitted. Diagnostic plots indicated a reasonable fit (e.g. no strong patterns were evident in the residuals and residuals were approximately normally distributed). The optimal model explained 59.2% of deviance and was as follows:

$$\begin{aligned} Y1 \sim 1 &+ s(\text{year}, \text{d.f.} = 8.9) + s(\text{depth}, \text{d.f.} = 8.3) \\ &+ s(\text{SST}, \text{d.f.} = 6.0) + s(\text{SST gradient}, \text{d.f.} = 8.4) \\ &+ \text{as factor(SST RV)}; \quad \text{AIC} = 1571. \end{aligned}$$

The model included non-linear effects of year ($P < 0.0001$), depth ($P = 0.0001$), SST ($P = 0.0001$) and gradient ($P = 0.0030$). SST RV was included as a nominal variable. None of the individual terms for SST RV was statistically significant but there was a trend for higher CPUE at higher SST RV. Replacing the nominal terms for SST RV with a linear term resulted in a slight increase in AIC but the term for SST RV was positive and significant ($P = 0.009$). The shapes of smoothers (Fig. 10) are complex but indicate that CPUE peaked at an SST of around 11 °C, a depth of around 160 m and SST gradient of around 250.

For hake CPUE in July, preliminary model fitting indicated that several high values were strongly influential and the CPUE data were therefore log-transformed before a Gaussian GAM with identity link function was fitted. Diagnostic plots indicated a reasonable fit. The optimal model explained 47.7% of deviance and was as follows:

$$\begin{aligned} \text{Y1} \sim 1 &+ s(\text{Year, d.f.} = 8.3) + s(\text{SST, d.f.} = 3.6) \\ &+ \text{as factor(SST RV)} + \text{depth}; \quad \text{AIC} = 134.6. \end{aligned}$$

The model included non-linear effects of year ($P < 0.0001$) and SST ($P < 0.0001$) and a negative linear effect of depth ($P < 0.0001$). Some intermediate SST RV values (0.22, 0.33, 0.56) were associated with higher CPUE than that at an SST RV of 0.11 ($P \leq 0.0316$) but no significant difference was seen between CPUE at SST RV = 0.11 and CPUE at the other SST RV values. SST gradient had no significant effect on CPUE and was dropped from the final model. The shapes of smoothers (Fig. 11) indicate that CPUE in July was lowest in 1997 and peaked at SST values of around 3° and 8 °C.

The optimal GAM model for CPUE in September, fitted assuming a quasi-Poisson distribution (a Poisson distribution with an extra parameter allowing for overdispersion) and a log-link, explained 50.9% of deviance. Diagnostic plots indicated a

Please cite this article in press as: Wang, J. et al., Remotely sensed local oceanic thermal features and their influence on the distribution of hake (*Merluccius hubbsi*) at the Patagonian shelf edge in the SW Atlantic, Fish. Res. (2006), doi:10.1016/j.fishres.2006.09.010

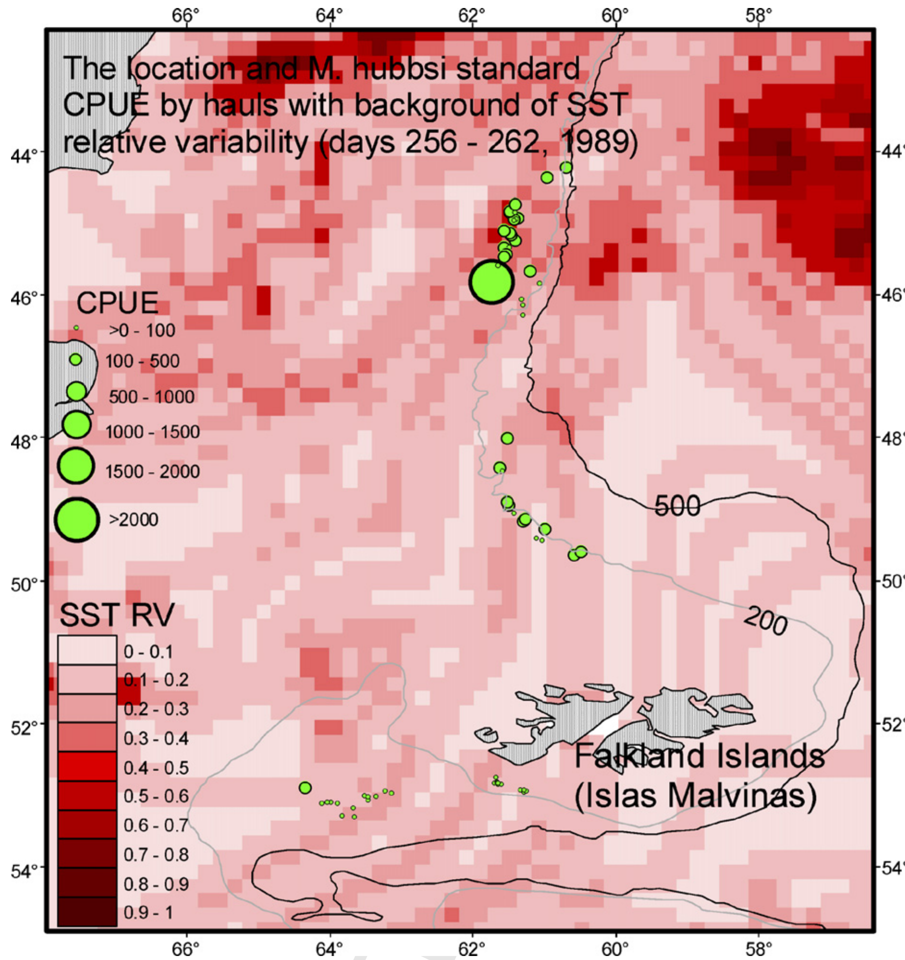

Fig. 8. The location and CPUE of fishing hauls with background of SST RV during the days from 256 to 262, 1989.

reasonable fit. The model had the form:

$$Y1 \sim 1 + s(\text{year}, \text{d.f.} = 8.5) + s(\text{depth}, \text{d.f.} = 2.5) + s(\text{SST},\ \text{d.f.} = 6.5) + s(\text{SST gradient},\ \text{d.f.} = 2.7) + \text{as factor(SST RV)};\quad \text{AIC} = 22,208.$$

The model included non-linear effects of year ($P < 0.0001$), depth ($P = 0.0006$), SST ($P < 0.0001$) and SST gradient, although the latter was not individually significant ($P = 0.1045$). Intermediate SST RV values (from 0.22 to 0.44) were associated with higher CPUE than an SST RV of 0.11 ($P \leq 0.0004$) but no significant difference was seen between CPUE at SST RV = 0.11 and CPUE at the highest SST RV values. The shapes of smoothers (Fig. 12) indicate that the partial effects of the various explanatory factors on CPUE i.e. taking account of the effects of all other explanatory variables were as follows: CPUE was lowest in 1991, declined at greater depths and peaked at an SST of around 8 °C. CPUE was lowest at intermediate values for SST gradient.

In summary, GAM results reveal strong and consistent effects of year, depth and SST on local CPUE. Additional predictive power was achieved by including SST gradient or SST RV. In April, both SST gradient and SST RV had significant effects while in July and September, only SST RV had a significant effect. Interestingly, although CPUE increased from low to intermediate values of SST RV, it was not generally highest at high SST RV values.

Table 2
Spearman's rank correlations for the relationships between CPUE, SST RV and SST gradient

	April			July			September		
	ρ	P-value	n	ρ	P-value	n	ρ	P-value	n
RV	0.41	<0.001	560	0.23	<0.001	271	0.14	0.001	561
Gradient	0.30	<0.001	560	0.13	0.039	271	0.05	0.277	561
Depth	−0.20	<0.001	435	−0.24	<0.001	259	−0.473	<0.001	299

Please cite this article in press as: Wang, J. et al., Remotely sensed local oceanic thermal features and their influence on the distribution of hake (*Merluccius hubbsi*) at the Patagonian shelf edge in the SW Atlantic, Fish. Res. (2006), doi:10.1016/j.fishres.2006.09.010

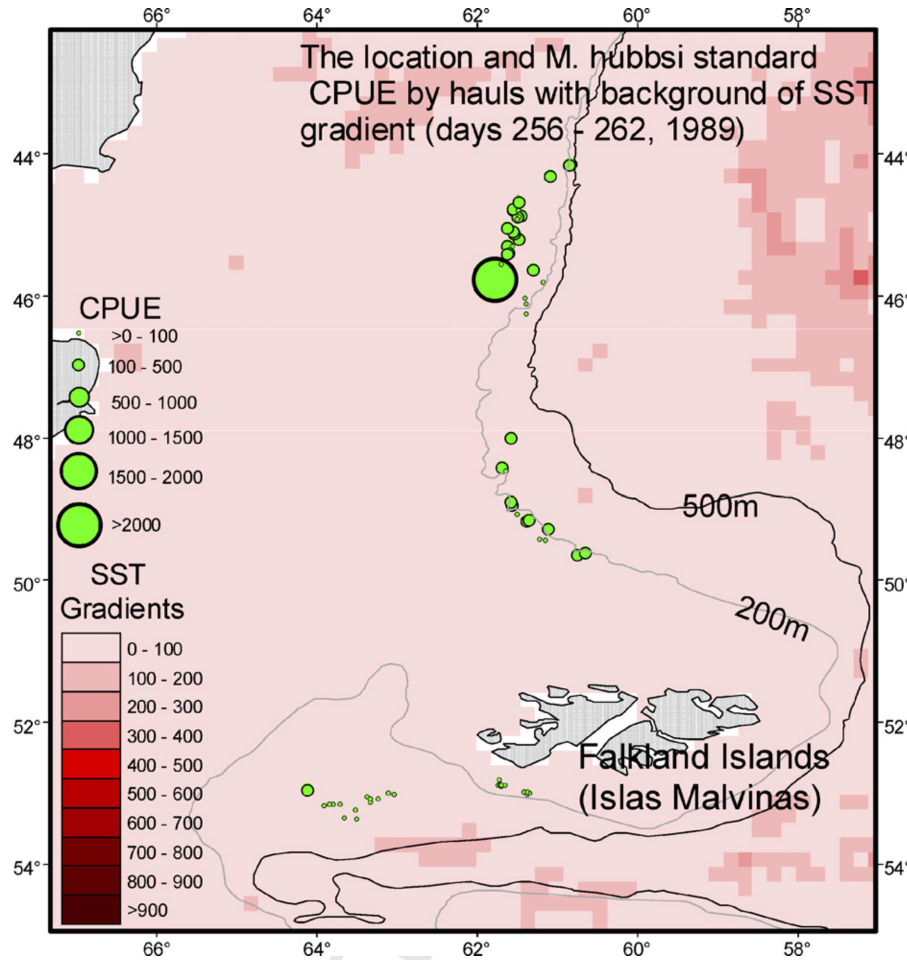

Fig. 9. The location and CPUE of fishing hauls with background of SST gradient during the days from 256 to 262, 1989.

4. Discussion

Local oceanic circulation features are areas of increased mixing both laterally and vertically. Such oceanic features may be caused by one, or a combination, of a wide and diverse range of forces, such as current convergence, wind, solar heating, bottom topography, tides, shelf breaks and geomorphic features (e.g. headlands, islands, and canyons) (Mann and Lazier, 1996, Acha et al., 2004).

The potential of remote sensed oceanographic data, especially SST and SST gradient, for locating aggregations of pelagic marine resources, especially fish, has been recognised for several years (Santos, 2000). In the present case, the study area is dominated by the Falkland (Malvinas) current (Fig. 1) (Peterson, 1992; Anderson and Rodhouse, 2001), which carries cold and nutrient-rich water of Antarctic origin from the APFZ, and flows northwards along the Patagonian Shelf edge, and a previous study reports that a strong Falkland (Malvinas) current has a positive influence on hake abundance in the study area (Podestá, 1989). In the vicinity of surface oceanic circulation features such as fronts, upwellings and gyres, the high concentration of zooplankton associated with the phytoplankton provides food for pelagic fish and cephalopod species (Rodhouse et al., 1996; González et al., 1997), which in turn provide food for species from higher trophic levels such as hake, which accumulate in such areas for food (Podestá, 1989).

SST gradient represents the maximum SST difference between a cell and its immediate neighbouring cells within a 3×3 neighbourhood. It has been widely used for detecting oceanic circulation features and to study the influence of oceanic circulation on fish distribution and abundance. SST gradient does not fully capture the heterogeneity of SST within the present study area, which is dominated by the influence of a single regional circulation current, the Falkland (Malvinas) current. Therefore, SST gradient data are mostly suitable for analysing regional oceanic circulation features, such as fronts, under circumstances where SST shows large quantitative changes. In contrast, SST RV provides information on local SST heterogeneity in a local neighbourhood (in the present example, a 3×3 block of cells, each cell covers 0.1758° longitude by 0.1758° latitude). It ignores the scale of quantitative variation in SST. Thus, SST RV as defined in this paper can be considered as a better indicator for detecting the presence of local thermal oceanic features under circumstances where SST has high spatial heterogeneity but quantitative differences are small. However, in the vicinity of regional oceanic circulation features such as fronts, SST typically shows both high spatial heterogeneity and high quantitative differences. In such areas, as

Please cite this article in press as: Wang, J. et al., Remotely sensed local oceanic thermal features and their influence on the distribution of hake (*Merluccius hubbsi*) at the Patagonian shelf edge in the SW Atlantic, Fish. Res. (2006), doi:10.1016/j.fishres.2006.09.010

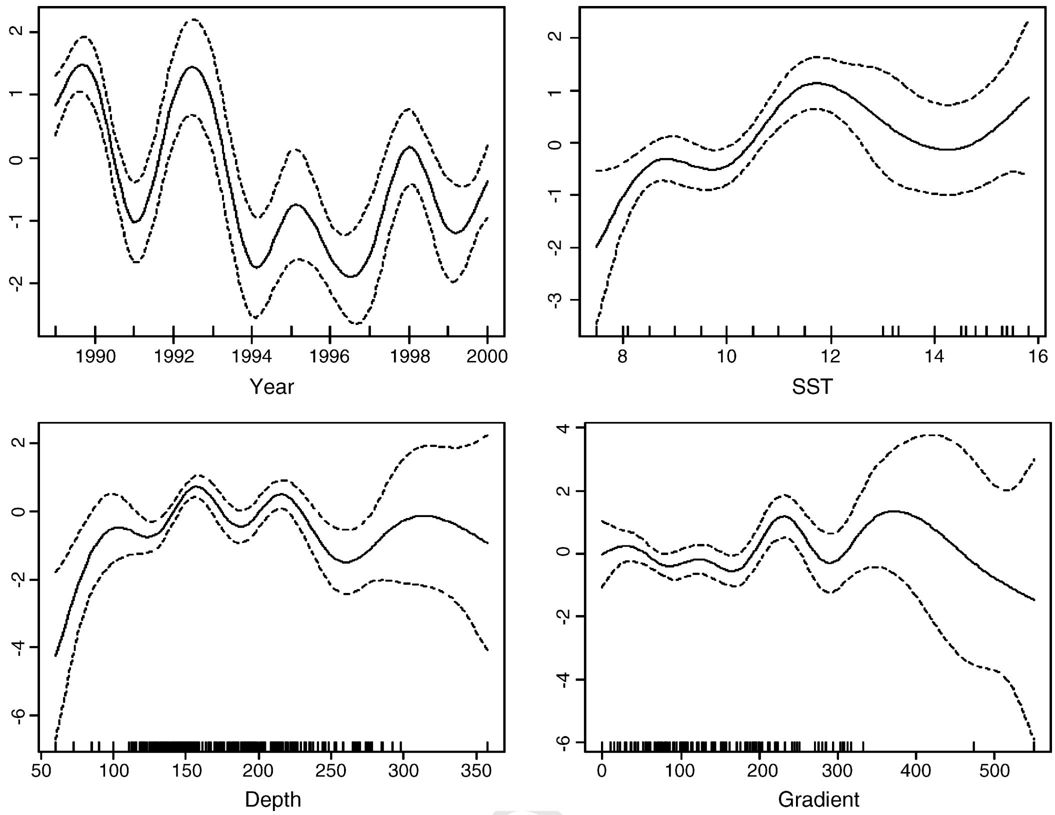

Fig. 10. Partial plots for GAMs fitted to CPUE data in April.

shown in Figs. 5 and 6, both SST gradient and SST RV have high values.

This study shows that SST RV was more closely related to local hake abundance in two out of three study months and we therefore infer that it captures some feature of environmental variation that is relevant to the fish. It may thus be suggested (although this analysis obviously provides no independent test), that SST RV is more useful for defining the presence of local thermal oceanic features. Within a single regional oceanic circulation feature area in the Patagonian shelf edge area, hake abundance, as measured by CPUE, has a positive association with local thermal oceanic features, although we did not investigate what causes these local thermal oceanic features. However, the analysis also reveals that fish abundance is low in areas with the highest values for SST RV. This may indicate that hake avoid areas with strong water turbulence. Cury and Roy (1989) indicated that the existence of an optimal environmental window in upwelling areas for pelagic fish recruitment, and in the case of a strong upwelling, turbulence is the limiting factor for recruitment.

M. hubbsi spawns from November through March. The peak spawning occurs in January (Macchi et al., 2004). During the studied months (April, July and September), they are travelling towards, and then present on, their feeding grounds (see Arkhipkin et al., 2003). Hake are reported to be associated with the shelf break front during their northward feeding migration

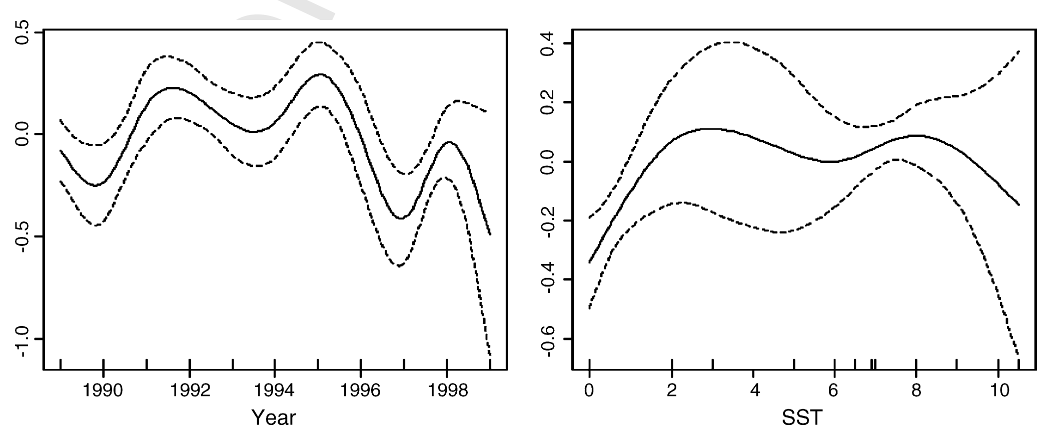

Fig. 11. Partial plots for GAMs fitted to CPUE data in July.

Please cite this article in press as: Wang, J. et al., Remotely sensed local oceanic thermal features and their influence on the distribution of hake (*Merluccius hubbsi*) at the Patagonian shelf edge in the SW Atlantic, Fish. Res. (2006), doi:10.1016/j.fishres.2006.09.010

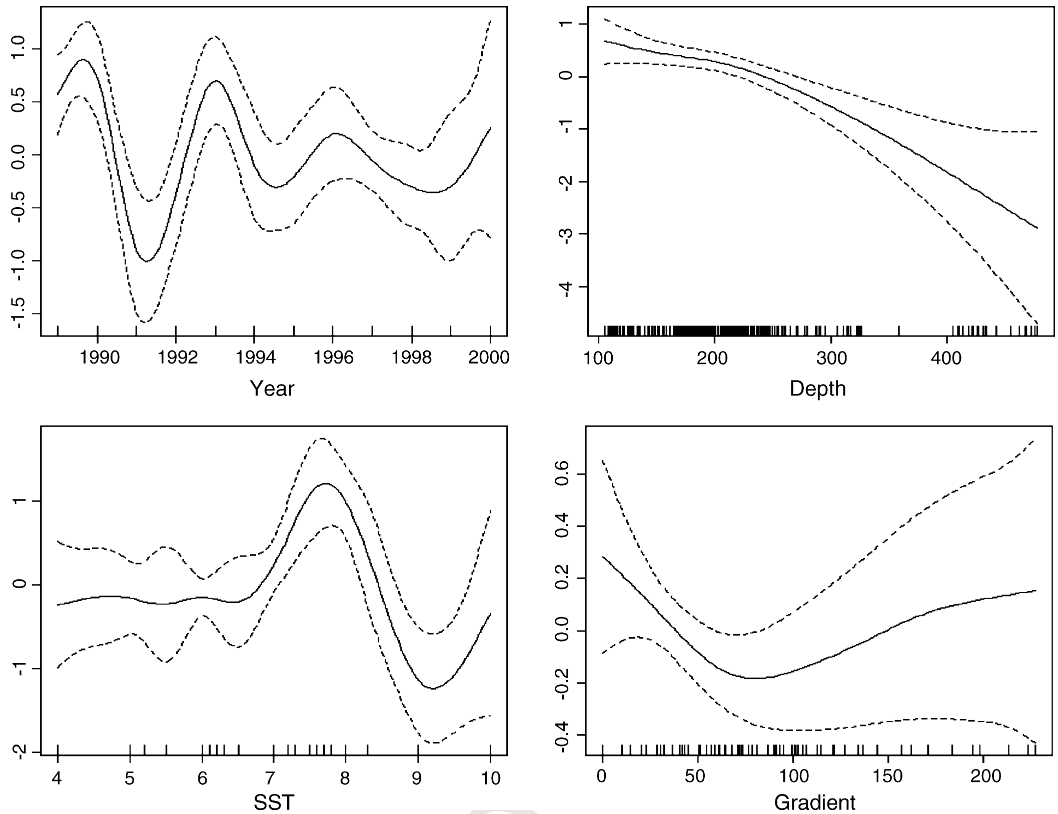

Fig. 12. Partial plots for GAMs fitted to CPUE data in September.

during the austral autumn, taking advantage of the presence of anchovy (*Engraulis anchoita*) (Brandhorst and Castello, 1971; Podestá, 1989; Acha et al., 2004). Our results suggest that hakes are associated with ocean surface features in their feeding grounds, as previously indicated by Podestá (1989), and that SST RV captures this behaviour more reliably than SST gradient.

The continental shelf of South America is characterised by the presence of a range of different frontal systems at different spatial scales (Acha et al., 2004). These frontal systems may be important at many stages of the hake's life. Thus, the eggs and early larvae of *M. hubbsi* are reportedly strongly associate with the shelf-break front (Ehrlich, 2000). On the Pacific coast, spawning in the congeneric Chilean hake *Merluccius gayi* is associated with an upwelling system and there appears to be retention of eggs and larvae in this system (Vargas et al., 1997; Vargas and Castro, 2001). Studies based on SST RV may therefore facilitate improved understanding the distribution of hake and other fish species throughout their life-cycle.

Acknowledgements

This research was supported by the European Commission's Directorate General for Fisheries under Study Project 99/16 and CRAFT project Q5CR-2002-71709. The authors wish to thank the IEO observers who collected the data. We would also like to thank the two anonymous referees for their comments to the manuscript.

References

Acha, E.M., Mianzan, H.W., Guerrero, R.A., Favero, M., Bava, J., 2004. Marine fronts at the continental shelves of austral South American physical and ecological processes. J. Mar. Syst. 44, 83–105.

Anderson, C.I.H., Rodhouse, P.G., 2001. Life cycles, oceanography and variability: ommastrephid squid in variable oceanographic environments. Fish. Res. 54, 133–143.

Arkhipkin, A.I., Middleton, D.A.J., Portela, J.M., Bellido, J.M., 2003. Alternative usage of common feeding grounds by large predators: the case of two hakes (*Merluccius hubbsi* and *M. australis*) in the Southwest Atlantic. Aquat. Living Resour. 16, 487–500.

Beaugrand, G., 2003. Long-term changes in copepod abundance and diversity in the north-east Atlantic in relation to fluctuations in the hydroclimatic environment. Fish. Oceanogr. 12, 270–283.

Bertolotti, M.I., Brunetti, N.E., Carreto, J.I., Prenski, L.B., Sanchez, R.P., 1996. Influence of shelf-break fronts on shellfish and fish stocks off Argentina. ICES CM 1996/S: 41.

Bezzi, S.I., Irusta, C.G., Simonazzi, M., Castrucci, R., Ibañez, P., 2000a. Sucesos biológicos y pesqueros del efectivo pesquero norte de merluza *Merluccius hubbsi* entre 39 degree y 41 degree. Frente Marítimo 18, 25–30.

Bezzi, S.I., Irusta, C.G., Ibanez, P., Simonazzi, M., Castrucci, R., 2000b. La pesquería argentina de merluza *Merluccius hubbsi* en la Zona Comun de Pesca. Periodo 1986–1996. Frente Marítimo 18, 7–23.

Brandhorst, W., Castello, J.P., 1971. Evaluación de los recursos de anchoíta (*Engraulis anchoita*) frente a la Argentina y Uruguay: 1. Las condiciones oceanográficas, sinopsis del conocimiento actual sobre la anchoíta y el plan para su evaluación. Contrib. Inst. Biol. Mar., Argentina 166, 1–63.

Brunet, C., Brylinski, J.M., Fronter, S., 1992. Productivity, photosynthetic pigments and hydrology in the coastal front of the Eastern English Channel. J. Plankton Res. 14, 1541–1552.

Burrough, P.A., 1986. Principles of Geographical Information Systems for Land Resources Assessment. Oxford University Press, New York, 193 pp.

Cole, J., 1999. Environmental conditions, satellite imagery, and clupeioid recruitment in the northern Benguela upwelling system. Fish. Oceanogr. 8, 25–38.

Cornillon, P., Stramma, L., 1985. The distribution of diurnal sea suface warming events in the Sargasso Sea. J. Geophys. Res. 90, 11811–11815.

Cury, P., Roy, C., 1989. Optimal environmental window and pelagic fish recruitment success in upwelling areas. Can. J. Fish. Aquat. Sci. 46, 670–680.

Ehrlich, M.D., 2000. Distribución y abundancia de huevos, larvas y juveniles de merluza (*Merluccius hubbsi*) en la Zona Común de Pesca Argentino–Uruguaya 1996–1998. Frente Marítimo 18, 31–44.

Garzoli, S.L., Garraffo, Z., 1989. Transports, frontal motions and eddies at the Brazil–Malvinas currents confluence. Deep-Sea Res. 36, 681–701.

González, A.F., Trathan, P.N., Yau, C., Rodhouse, P.G., 1997. Interactions between oceanography, ecology and fishery biology of the ommastrephid squid *Martialia hyadesi* in the South Atlantic. Mar. Ecol. Prog. Ser. 152, 205–215.

González-Quirós, R., Pascual, A., Gomis, D., Anadón, R., 2004. Influence of mesoscale physical forcing on trophic pathways and fish larvae retention in the central Cantabrian Sea. Fish. Oceanogr. 13, 351–364.

Grioche, A., Koubbi, P., 1997. A preliminary study of the influence of a coastal frontal structure on ichthyoplankton assemblages in the English Channel. ICES J. Mar. Sci. 54, 93–104.

Hardman-Mountford, N.J., McGlade, J.M., 2003. Seasonal and interannual variability of oceanographic processes in the Gulf of Guinea: an investigation using AVHRR sea surface temperature data. Int J. Remot. Sens. 24, 3247–3268.

Kimura, S., Nakata, H., Okazaki, Y., Kasai, A., 1998. Biological production in meso-scale eddies caused by frontal disturbances of the Kuroshio and the Kuroshio Extension. ICES CM 1998/R:9.

Koubbi, P., Ibanez, F., Duhamel, G., 1991. Environmental influences on spatio-temporal oceanic distribution of ichthyoplankton around the Kerguelen Islands (Southern Ocean). Mar. Ecol. Prog. Ser. 72, 225.

Lafuente, J.G., Vargas, J.M., Criado, F., García, A., Delgado, J., Mazzola, S., 2005. Assessing the variability of hydrographic processes influencing the life cycle of the Sicilian Channel anchovy, Engraulis encrasicolus, by satellite imagery. Fish. Oceanogr. 14, 32–46.

Macchi, G.J., Pájaro, M., Ehrlich, M., 2004. Seasonal egg production pattern of the Patagonian stock of Argentine hake (*Merluccius hubbsi*). Fish. Res. 67, 25–38.

Mann, K.H., Lazier, J.R.N., 1996. Dynamics of Marine Ecosystems. Biological–Physical Interactions in the Oceans, 2nd ed. Blackwell, Cambridge, USA.

Martínez, J.P., Iglesias, S., Ramilo, G., 1997. Pesquerías de mayor interés para la flota española en el Atlántico Sudoccidental (ATSO). Informes Técnicos del Instituto Español de Oceanografía 165, 1–45.

Murphy, E.J., Watkins, J.L., Reid, K., Trathan, P.N., Everson, I., Croxall, J.P., Priddle, J., Brandon, M.A., Brierley, A.S., Hofmann, E., 1998. Interannual variability of the South Georgia marine ecosystem: biological and physical sources of variation in the abundance of krill. Fish. Oceanogr. 7, 381–390.

Olson, D.B., Mariano, A.J., Ashjian, C.J., Peng, G., Nero, R.W., Podestá, G.P., 1994. Life on the edge: marine life and fronts. Oceanography 7, 52–60.

Peterson, R.G., 1992. The boundary currents in the western Argentine basin. Deep-Sea Res. 39, 623–644.

Peterson, R.G., Whiteworth III, T., 1989. The sub-Antarctic and Polar fronts in relation to deep water masses through the southwestern Atlantic. J. Geophys. Res. 94, 10817–10838.

Podestá, G.P., 1989. Migratory pattern of Argentine hake *Merluccius hubbsi* and oceanic processes in the southwestern Atlantic Ocean. Fish. Bull. 88, 167–177.

Reid, D.G., 2001. SEFOS–shelf edge fisheries and oceanography studies: an overview. Fish. Res. 50, 1–15.

Rodhouse, P.G., Prince, P.A., Trathan, P.N., Hatfield, E.M.C., Watkins, J.L., Bone, D.G., Murphy, E.J., White, M.G., 1996. Cephalopods and mesoscale oceanography at the Antarctic polar front: satellite tracked predators locate pelagic trophic interactions. Mar. Ecol. Prog. Ser. 136, 37–50.

Sacau, M., Pierce, G.J., Wang, J., Alexander, I., Arkhipkin, A.I., Portela, J., Brickle, P., Santos, M.B., Zuur, A.F., Cardoso, X., 2005. The spatio-temporal pattern of Argentine shortfin squid Illex argentinusabundance in the southwest Atlantic. Aquat. Living Resour. 18, 361–372.

Santos, A.M.P., 2000. Fisheries oceanography using satellite and airborne remote sensing methods: a review. Fish. Res. 49, 1–20.

Stramma, L., Cornillon, P., Weller, R.A., Price, J.F., Briscoe, M.G., 1986. Large sea surface temperature variability: satellite and *in situ* measurement. J. Phys. Oceanogr. 16, 827–837.

Trathan, P.N., Brierley, A.S., Brandon, M.A., Bone, D.G., Goss, C., Grant, S.A., Murphy, E.J., Watkins, J.L., 2003. Oceanographic variability and changes in Antarctic krill (*Euphausia superba*) abundance at South Georgia. Fish. Oceanogr. 12, 569–583.

Turrell, W.R., 1992. New hypotheses concerning the circulation of the northern North Sea and its relation to North Sea fish stock recruitment. ICES J. Mar. Sci. 49, 107–123.

Ullman, D.S., Cornillon, P.C., 2000. Evaluation of front detection methods for satellite-derived SST data using in situ observations. J. Atm. Ocean. Technol. 17, 1667–1675.

Valavanis, V.D., Katara, I., Palialexis, A., 2005. Marine GIS: Identification of mesoscale oceanic thermal fronts. Int. J. Geogr. Informat. Sci. 19, 1131–1147.

Vargas, C.A., Castro, L.R., 2001. Spawning of the Chilean hake (*Merluccius gayi*) in the upwelling system off Talcahuano in relation to oceanographic features. Sci. Mar. 65, 101–110.

Vargas, C.A., Valenzuela, G.S., Núñez, S.P., Arcos, D.F., 1997. Role of oceanographic and topographic factors in the retention of hake (*Merluccius gayi gayi* Guichenot, 1848) larvae in the upwelling system off central-southern Chile. Arch. Fish. Mar. Res. 45, 201–222.

Waluda, C.M., Trathan, P.N., Rodhouse, P.G., 1999. Influence of oceanographic variability on recruitment in the *Illex argentinus* (Cephalopoda: Ommastrephidae) fishery in the South Atlantic. Mar. Ecol. Prog. Ser. 183, 159–167.

Waluda, C.M., Rodhouse, P.G., Trathan, P.N., Pierce, G.J., 2001. Remotely sensed mesoscale oceanography and the distribution of *Illex argentinus* in the South Atlantic. Fish. Oceanogr. 10, 207–216.

Wang, J., Pierce, G.J., Boyle, P.R., Denis, V., Robin, J.-P., Bellido, J.M., 2003. Spatial and temporal patterns of cuttlefish (*Sepia officinalis*) abundance and environmental influence—a case study using trawl fishery data in French Atlantic coastal, English Channel, and adjacent waters. ICES J. Mar. Sci. 60, 1149–1158.

Zheng, X., Pierce, G.J., Reid, D.G., Jolliffe, I.T., 2002. Does the North Atlantic current affect spatial distribution of whiting? Testing environmental hypotheses using statistical and GIS techniques. ICES J. Mar. Sci. 59, 239–253.